Cell Reports
Physical Science

CellPress
OPEN ACCESS

Article

Electrochemical polymerization of polyhydrocarbons by reductive dehalogenation of chlorinated methanes

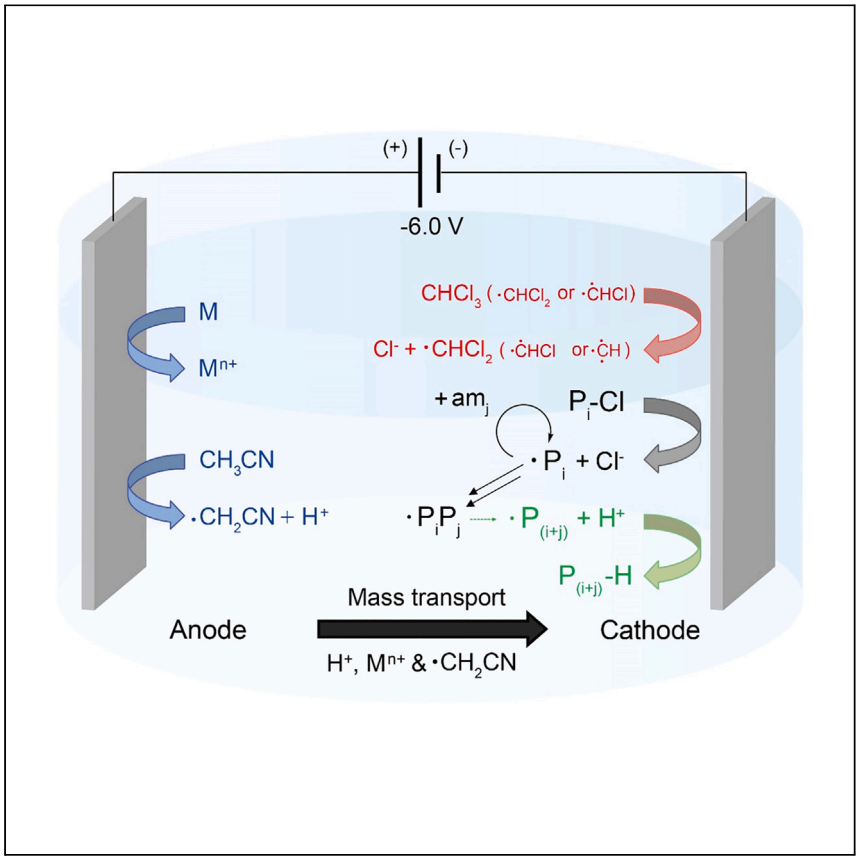

Electrochemistry could be a useful technique for mild polymer synthesis, but the reactions are often challenging to understand. Here, Seo et al. investigate the mechanism of the electrochemical polymerization of polyhydrocarbons, identifying the initiation, propagation, and termination processes with combined electrochemical and spectroscopic techniques.

Jae Hong Seo, Rajmohan Rajendiran, Sun Hwa Lee, Rodney S. Ruoff

sunhlee@ibs.re.kr (S.H.L.)
rsruoff@ibs.re.kr (R.S.R.)

Highlights

Key mechanistic steps in the electrochemical polymerization of polyhydrocarbons are probed

Deprotonation and reduction of CH_3CN and CH_xCl_y are observed at the anode and cathode

Propagation is studied via electrochemical techniques combined with NMR and FT-IR

Proof of termination step is obtained using isotope-labeled chemicals

Seo et al., Cell Reports Physical Science 4, 101373
April 19, 2023
https://doi.org/10.1016/j.xcrp.2023.101373

Cell Reports
Physical Science

CellPress
OPEN ACCESS

Article

Electrochemical polymerization of polyhydrocarbons by reductive dehalogenation of chlorinated methanes

Jae Hong Seo,[1,2] Rajmohan Rajendiran,[1] Sun Hwa Lee,[1,*] and Rodney S. Ruoff[1,2,3,4,5,*]

SUMMARY

Electrochemistry is a useful technique for mild synthesis of polymers, but the mechanisms of electrochemical polymerization are challenging to fully understand. Here, we focus on understanding the reaction mechanisms during the electrochemical polymerization of polyhydrocarbons. The overall synthetic pathway for hyperbranched polyhydrocarbons is investigated using electrochemical methods combined with spectroscopy, namely nuclear magnetic resonance (NMR) and Fourier transform infrared (FT-IR). The oxidation and reduction occurring on the anode and cathode are investigated by cyclic voltammetry and NMR analyses to distinguish the functions of each electrode at the reaction initiation. Real-time FT-IR measurements during electrochemical polymerization are used to decipher the propagation steps. The termination by various suppliers of hydrogen atoms (such as aqueous hydrochloric acid) is examined via NMR spectroscopy using deuterium-labeled acetonitrile and chloroform. The participation of chlorinated methanes and of the solvent acetonitrile in the electrochemical polymerization is interrogated. Overall, these findings advance understanding of the key steps in the polymerization reaction.

INTRODUCTION

Electrochemistry is a growing typical method for green and mild reactions.[1] It is now a versatile method for organic synthesis, energy storage, sensing, conversion technologies, surface science, pollutant removal, and real-time analysis/screening.[2–12] Unlike a conventional wet-chemical reactions, it does not require harsh oxidizing and reducing agents in the reaction. As a result, the formation of undesired by-products can be minimized.[13] Owing to these characteristics, organic synthesis by electrochemical reactions, including electrochemical polymerization, has been reported.[14–19] Many electrochemical studies on the hydrodehalogenation of halogenated hydrocarbons have been reported.[20–22] However, electrochemical polymerization using chlorinated hydrocarbons has not been thoroughly investigated. We have previously reported on the synthesis[23] and structural analysis[24] of polyhydrocarbons (PHCs) through electrochemical polymerization. Here, mechanistic analysis is used to understand the reaction processes in terms of radical polymerization.

The electrochemical reductive cleavage of a series of chlorinated hydrocarbons, such as chlorinated methanes, chloroaromatics, and chloroalkenes, has been investigated using various electrodes, including Ag, Pt, Cu, Pd, Ni, Mo, Fe, glassy carbon (GC), and stainless steel (SS).[22,25–27] The Gennaro group reported the electrocatalytic reduction of volatile chlorinated methanes on the Cu, Pd, and GC/Ag

[1]Center for Multidimensional Carbon Materials (CMCM), Institute for Basic Science (IBS), Ulsan 44919, Republic of Korea

[2]Department of Chemistry, Ulsan National Institute of Science of Technology (UNIST), Ulsan 44919, Republic of Korea

[3]School of Energy and Chemical Engineering, Ulsan National Institute of Science of Technology (UNIST), Ulsan 44919, Republic of Korea

[4]Department of Materials Science and Engineering, Ulsan National Institute of Science of Technology (UNIST), Ulsan 44919, Republic of Korea

[5]Lead contact

*Correspondence: sunhlee@ibs.re.kr (S.H.L.), rsruoff@ibs.re.kr (R.S.R.)

https://doi.org/10.1016/j.xcrp.2023.101373

electrodes.[4,28–30] Fe, Ni, and Mo electrodes also reportedly exhibited high faradaic efficiency for the reductive cleavage of chlorinated hydrocarbons.[21] Based on the perceived formation of hydrocarbon radicals by electrochemical reactions, there are reports of electrochemical polymerization using chloroform ($CHCl_3$), hexachloroethane (C_2Cl_6), and 1,1,1-trichloroethane (CH_3CCl_3).[19,31,32] The authors did not report any investigation of the reaction mechanism(s) related to electrocatalytic reduction and polymerization.

Cyclic voltammetry (CV) involves monitoring the current response during continuous potential cycling. It provides information about the thermodynamics of the redox process, the energy levels of the analyte, and the kinetics of the electron transfer reaction. Here, real-time analysis of the oxidized or reduced species has been accomplished using electrochemical analysis combined with nuclear magnetic resonance (NMR), Fourier transform infrared (FT-IR), and UV-visible (UV-vis) spectroscopy. CV shows high chemical specificity and detects dynamic processes, such as metastable and short-lived phases. Gray et al. reported a change in lithium and sodium battery states by *in situ* NMR combined with electrochemistry.[33–35] Kato et al. reported tracking the movement of electrons through an *in situ* FT-IR method combined with electrochemistry.[36] The Shi-Gang Sun group reported using both electrochemical-NMR (EC-NMR) and *in situ* FT-IR methods to improve the analysis of intermediate species in the formation of glycerol. They reported the changes in chemical structure according to potential or reaction time.[37] For CV combined with *in situ* NMR, there are three reported challenges: (1) changing sample conditions, (2) NMR signal broadening, and (3) EC-NMR circuit interference.[34] We thus chose to measure both FT-IR and ^{1}H-NMR within a short period of time after extracting a volume of the solution (according to the reaction time) to study the evolution of the electrochemical reaction, without changing the sample conditions in NMR and thus eliminating the effect of circuit interference.

Here, we introduce a reaction pathway to electrochemically synthesize PHC using chlorinated hydrocarbons in three steps: (1) initiation, (2) propagation, and (3) termination, and we have also studied the role of acetonitrile (CH_3CN) as a solvent—which we learned also participates in certain reactions. In our previous research, we reported that the molecular structure and composition of the obtained PHC varied depending on whether dichloromethane (CH_2Cl_2), $CHCl_3$, or carbon tetrachloride (CCl_4) was used as the monomer.[23,24] In an attempt to understand the initiation process, the cathode and anode redox reactions were separately analyzed using the CV method. Combining FT-IR and NMR analyses was found to be very useful in tracing intermediate products during the propagation process. The hydrogen and carbon incorporation was studied using a deuterated monomer ($CDCl_3$), a deuterated solvent (CD_3CN), and ^{13}C-labeled chloroform ($^{13}CHCl_3$). By using isotope-labeled monomers, we also studied the role of CH_3CN during the electrochemical synthesis of PHC. Note that hydrochloric acid HCl(aq) was typically used for purification. We observed an electrochemical reduction utilizing CH_2Cl_2, $CHCl_3$, and CCl_4 as monomers and here suggest how the electrochemical synthesis of PHC under our conditions progress from each monomer in the presence of acetonitrile as solvent. And in particular, we focus on the monomer $CHCl_3$, as we chose to study it most extensively.

RESULTS AND DISCUSSION

Synthesis of PHCs

The PHCs were synthesized by an electrochemical polymerization process using CH_2Cl_2, $CHCl_3$, and CCl_4 as monomers and CH_3CN as the solvent.[23] Lithium

$$M \longrightarrow M^{n+} + ne^-$$

Scheme 1. Oxidation of metals at the SS316 anode

hexafluorophosphate ($LiPF_6$) acted as an electrolyte in CH_3CN. The chlorinated methane solutions were contained in an electrochemical cell composed of working, counter, and reference electrodes ($Ag/AgNO_3$), with stirring by a magnetic bar to try to keep the solution homogeneous.

Oxidation at the anode during the initiation step

Chlorinated methanes are not electrically conductive, making electrolysis difficult. SS316 electrodes were used as the cathode and anode to activate the dissociation of chlorinated methanes. The oxidation of metals from the SS316 anode promoted electron transfer by increasing the electroconductivity of the reaction solution. The oxidation of the electrode is shown in Scheme 1.

SS316, which was used as the electrode, is stated to contain Fe, Ni, Cr, Mo, and Mn. Fe and Ni reportedly promote reducing chlorinated hydrocarbons (in studies to eliminate volatile organic compounds [VOCs]).[21] When measuring the CV of the reaction solution containing a particular monomer, CH_3CN, and $LiPF_6$, at potentials from 0.00 to 6.00 V, the current was proportionally increased due to the oxidation of the anode. Figures S1A–S1C show that the oxidation of the three monomers was commonly observed. CH_3CN was stable in the first cycle between 0.00 and 1.45 V, thus within its well-known "solvent window," for each of the 3 monomers. However, the solvent window region disappeared after the first cycle. We attempted to evaluate any chemical change in CH_3CN in our electrochemical cell at applied potentials outside the solvent window of CH_3CN. We thus explored the reduction process using CH_3CN with $LiPF_6$ alone, with no monomer. The yellow box in Figure S2A shows that reduction occurred at −2.68 V in the first cycle, but no reduction peaks were observed after the second cycle. The absolute current value at −6.00 V decreased as the cycle progressed. CH_3CN formed by-products, and this caused the electrode surface to be passivated.[38] ^{1}H-NMR spectra were obtained for samples collected right after reaching 0 V (in red box) at each cycle (1, 5, 10, 30, and 50 cycles), as shown in Figure S2B. As the cycle ended, it was found that the product derived from CH_3CN had ^{1}H-NMR peaks at 3.48 and 3.93 ppm. These peaks were attributed to the dimers or oligomers of CH_3CN.[39] The hydrocarbon groups marked in the gray box of Figure S2B were observed owing to the addition of $LiPF_6$ in CH_3CN (see Figure S2C). When $LiPF_6$ was added to the solvent, the intensity of the hydrocarbon peak was increased. Chronoamperometry (CA) of CH_3CN revealed that the absolute value of the current decreased to −0.13 mA from 0 to 2 h and remained constant until the end of the reaction, as shown in Figure S3A. The ^{1}H- and ^{13}C-NMR results in Figures S3B and S3C show that the dimer or oligomer of CH_3CN was synthesized on the cathode. The deposited products appeared to interrupt the redox reaction on the cathode.[39–41] The hydrogen atoms of the methyl group might be predominantly dissociated. The radical formation from CH_3CN is displayed in Scheme 2.

The metal ions generated at the anode, activated CH_3CN, and protons were mass transported to the cathode by diffusion and migration.

$$CH_3CN \longrightarrow \cdot CH_2CN + H^+ + e^-$$

Scheme 2. Oxidation of CH_3CN on the anode

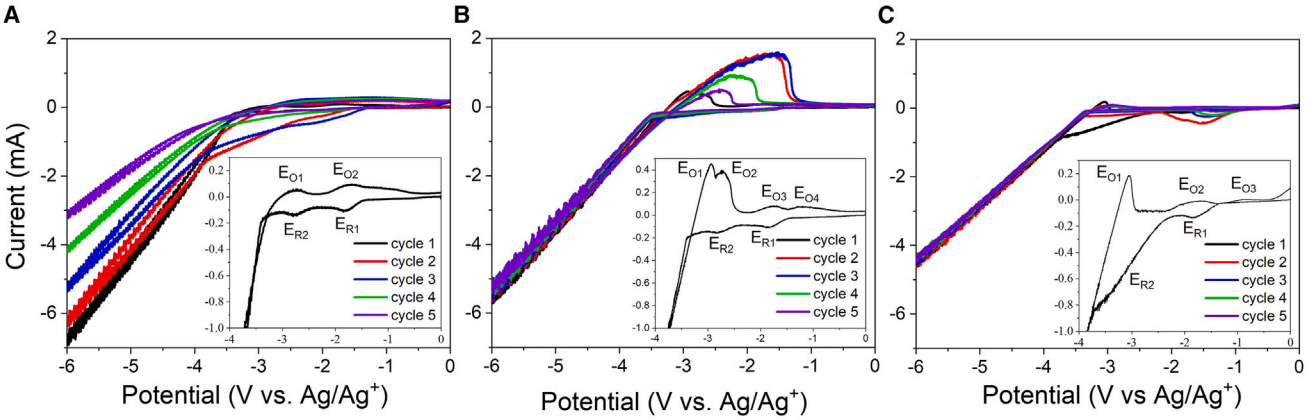

Figure 1. CV curves detailing reaction at the cathode

CV results of the cathode using 6.2 M (A) CH_2Cl_2, (B) $CHCl_3$, and (C) CCl_4 with CH_3CN and 23 mmol $LiPF_6$. The inset graphs show the high magnification of each first cycle. The potential was swept from 0 to −6 V five times with a scan rate of 10 mV/s at room temperature.

Reduction at the cathode during the initiation step

The voltammograms for CH_2Cl_2, $CHCl_3$, and CCl_4 in CH_3CN were determined at a scan rate of 10 mV/s from 0.00 to −6.00 V, as shown in Figure 1. The first (E_{R1}) and second (E_{R2}) reduction peaks at −1.83 and −2.78 V, respectively, indicated the cleavage of the C–Cl bond in the first cycle for the CH_2Cl_2 solution (see Figure 1A). The CH_2Cl_2 monomer, the electrolyte, and the solvent, all decomposed when the potential dropped below −3.37 V, which is beyond the electrochemical stability of CH_3CN, and the absolute current increased. The two oxidation peaks, E_{O1} and E_{O2}, appeared at −2.73 and −1.69 V, respectively, when the potential was reversed. These peaks indicate the oxidation of the decomposed monomer and solvent species.

Unlike the peaks observed in Figures 1B and 1C, there were no oxidation peaks representing the cathodic stripping effect.[42] The absolute current values of CH_3CN and CH_2Cl_2 reactions at −6.00 V decreased linearly with time when holding at −6.00 V. This decrease suggested that cathodic stripping, including the lithium component, did not occur as the solid-electrolyte interphase (SEI) layer on the cathode surface became thicker.[43–47] In contrast, the absolute current values of the $CHCl_3$ and CCl_4 solutions at −6.00 V were constant in time; this suggests that the Li and other metal components from the SS316 electrode were stripped off the cathode, and then the SEI layer was ruptured.

After each of the CV cycles, the intensity of the C–Cl reduction peaks increased and the peaks broadened owing to the reduction of CH_2Cl_2, but the reduction rarely occurred after the third cycle. This appeared to be related to the decrease in the absolute current at −6.00 V as the CV cycles proceeded. The electrochemical reactions were gradually interrupted by the by-product deposited on the cathode. The first CV cycle of $CHCl_3$ has E_{R1} and E_{R2} at −1.85 and −2.82 V, respectively. This is associated with the removal of two chlorine atoms from $CHCl_3$, resulting in the formation of the intermediate species, *CHCl (* = radical). The absolute values of reduction potentials were slightly higher than the dechlorination potentials of CH_2Cl_2 (see Figure 1B). The dechlorinated intermediate compounds were further reduced at the higher negative potential of −3.40 V. The residual C–Cl bonds in the activated monomer were also dissociated at −3.40 V.[22,28,29] Once the potential was −3.40 V, Li^+ from the electrolyte was reduced and deposited on the SS316 cathode and formed a

$$CH_nCl_{4-n} + me^- \longrightarrow \cdot CH_nCl_{4-n-m} + mCl^-$$

Scheme 3. Reduction of chlorinated methane on the cathode

black/brown passivation layer on the cathode, with decomposed solvent, intermediate monomer compound(s), or both. The black/brown layer was composed of 35.8 atom % carbon, 18.4 atom % lithium, 17.0 atom % oxygen, 9.57 atom % nitrogen, 8.93 atom % chlorine, 5.16 atom % silicon, 3.60 atom % iron, and 1.48 atom % chromium by X-ray photoelectron spectroscopy (XPS), as shown in Figure S4. As the potential reached −6.00 V, the absolute value of the current did not decrease as more cycles were imposed, unlike the CV depicted in Figure 1A. The relatively large E_{O1} and E_{O2} in the reversed scan appeared at the potentials −2.94 and −2.72 V, which indicated the stripping of Li from the passivation layer, and E_{O3} and E_{O4} at −1.76 and −1.23 V corresponded to the oxidation of solvent and partially activated monomers, respectively. During the subsequent cycles, these oxidation peaks, including those for Li stripping from the passivation layer, shifted and merged to form a single oxidation peak.

We switched the electrolyte to tetrabutylammonium hexafluorophosphate ($TBAPF_6$) to test the Li stripping phenomenon. No strong oxidation peak was observed at the potential of −3.40 V (see Figure S5). However, employing $TBAPF_6$ instead of $LiPF_6$ resulted in a smaller solvent window for CH_3CN. That is, there is improved stability of acetonitrile with the Li electrolyte.

The first cycle in the CV graph of CCl_4 showed that the first reduction peak appeared at −1.83 V related to the first C–Cl bond cleavage, and further chlorine reduction peaks from −2.33 to −3.75 V were not distinguishable. After reaching −3.70 V, the electrolyte and acetonitrile began to decompose, as shown in Figure 1C. The first oxidation peak at −3.00 V indicates Li extraction from the passivation layer. The second and third oxidation peaks at −1.82 and −0.87 V are due to the oxidation of decomposed solvent and monomers. The first reduction peak, E_{R1}, shifted to −1.53 V with increasing current intensity. As the cycles progressed, it shifted toward −1.20 V. Based on the results for the cathode, it can be deduced that the chlorinated hydrocarbon monomers were reduced by C–Cl bond cleavage, which is expressed as outlined in Scheme 3.

We have previously reported that the yield of PHCs linearly increased with the reaction time.[23] In particular, the yield increased as the absolute value of the current increased. This might mean that the synthesis of PHCs proceeded as a chain-growth process.

Propagation step at the cathode

FT-IR spectra were obtained (sample preparation described below) in time steps as the experiment progressed in an attempt to observe the propagation of the activated monomer on the cathode. The results are depicted in Figure 2A. We particularly focused on the use of $CHCl_3$ as a monomer to delve more deeply into various issues related to the growth of PHCs as a function of time. The samples were prepared by placing KBr pellets in the extracted solution according to the reaction time. All KBr pellets had the same thickness and were immersed in the extracted solution for 1 min. The FT-IR spectrum of the sample before electrochemical polymerization (0 h, black line) showed the IR pattern of oxidized $LiPF_6$ when exposed to oxygen and moisture.[48] It was observed that the oxidation of CH_3CN and the electrolytes became stronger with time. The peak intensities at 2,325 and 2,240 cm^{-1}

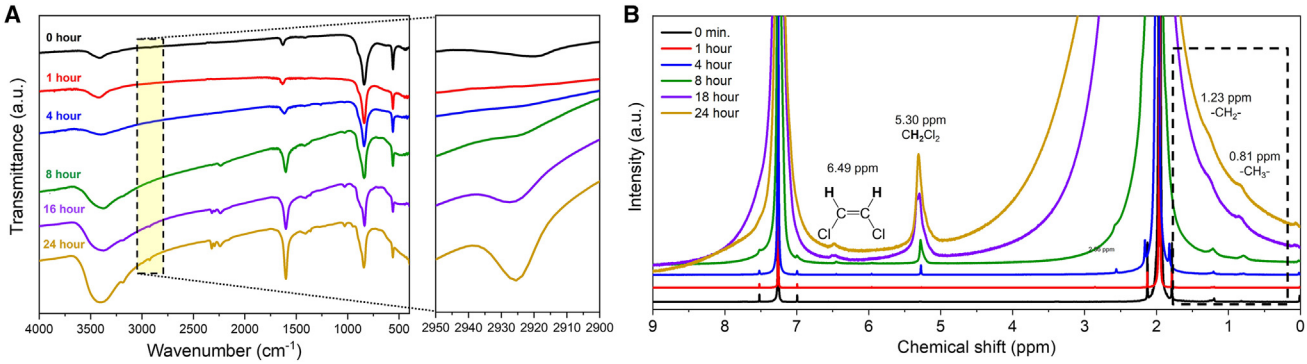

Figure 2. Identification of propagation steps in the electrochemical polymerization

(A) FT-IR spectra in the range 4,000–400 cm^{-1}, obtained by extracting solutions from the cell under electrochemical polymerization using $CHCl_3$ at specific times (0, 1, 4, 8, 16, and 24 h) and high-magnitude regions from 2,950 to 2,900 cm^{-1} in the yellow box.

(B) ^{1}H-NMR spectra using the extracted solution according to the reaction time (0, 1, 4, 8, 18, and 24 h). $CHCl_3$ was reduced to the polymer (or oligomer) of hydrocarbons at 0.81 ppm in the methyl group and 1.23 ppm in the methylene group.

increased, indicating the formation of by-products with nitrile groups from CH_3CN. The IR pattern for the 2,950 to 2,900 cm^{-1} region (yellow box) shows that the peaks in the C-H stretch region steadily increased, a clear indication that the polymer gradually formed over time.

The hydrocarbon peaks at 0.81 (methyl group) and 1.23 ppm (methylene group) increased with the reaction time, as shown by the NMR spectra of each solution (Figure 2B). CH_2Cl_2 and dichloroethene, a dimer of $CHCl_3$, were also formed, and simultaneous hydrogenation, not polymerization, occurred. However, as the reaction progressed, the NMR peaks of the monomer and the solvent broadened, due to Knight shift,[34,49,50] and the by-product from CH_3CN appeared at 2.56 ppm. When CA was performed at −3 V.00 for 24 h, the potential was within the solvent window of CH_3CN, and the absolute value of the current was constant and close to 0, as shown in Figure S6: the polymerization did not occur even though −3.00 V is over the reduction potential of the monomer; thus, CH_3CN plays a role in PHC synthesis, which will be addressed in more detail in the section about termination below. Based on the experimental data of the product reported earlier,[24] we know that the C–Cl bonds of the chlorinated monomers are randomly cleaved "on" the cathode, and each of the activated monomers is thus irregularly making covalent bonds (propagation proceeds) when the potential exceeds the solvent window of CH_3CN. The propagation scheme for the reaction of activated monomers with radicals is as shown in Scheme 4.

Investigation of termination step using deuterated chemicals

After purification ("work up") using hydrochloric acid (HCl), the empirical formula of PHC using $CHCl_3$ was close to CH_2.[24] This empirical formula indicates that employing the monomer of $CHCl_3$ increased the ratio of hydrogen atoms per carbon atom. Thus, there had to be other (or another) hydrogen atom suppliers. There are several possible candidates: (1) CH_3CN, which is used as the solvent, (2) HCl(aq), used to remove metal impurities during the purification process, and (3) moisture in the air. We thus synthesized PHCs using deuterated acetonitrile (CD_3CN) and deuterated chloroform ($CDCl_3$). The kinetic isotope effect (KIE) must be considered: heavier isotopes typically have a lower reaction rate.[51,52] Indeed, we found a difference in yield: (1) the yield for $CHCl_3$ with CH_3CN was 2.28%,[23] (2) the yield for $CDCl_3$ with CH_3CN was 2.18%, (3) the yield for $CHCl_3$ with CD_3CN was 0.49%, and (4) the yield for $CDCl_3$ with CD_3CN was 0.39%.

$$\cdot P_i + am_j \longrightarrow \cdot P_{(i+j)}$$

Scheme 4. Propagation process of chlorinated methanes on the cathode

P represents the propagated oligomer or polymer and am represents the activated monomer. The activated monomers are *$CHCl_2$, *CHCl, and *CH from $CHCl_3$. (*i* and *j* are integers, and ● represents radicals.)

The molecular weight of the deuterated PHC (2, 3, and 4) was too small to be detected by gel permeation chromatography multi-angle light scattering (GPC-MALS) when the deuterated chemical was used. We thereby learned that CH_3CN plays an important role in the electrochemical reaction. We compared ^{1}H-NMR spectra to determine the hydrogen atom supplier (see Figure 3).

These five ^{1}H-NMR spectra were from the use of the same solution concentration and normalized based on the NMR solvent peak ($CDCl_3$, δ = 7.26 ppm). Assuming that the NMR solvent peak area (δ = 7.26 ppm) is 1, the integration of the hydrocarbon region from 0.50 to 1.80 ppm is 153.18, as shown in Figure 3A. When $CDCl_3$ was used instead of $CHCl_3$, a sharp methyl peak at 0.88 ppm, a methylene peak at 1.25 ppm, and a methine peak at 1.58 ppm were observed, as shown in Figure 3B. The integration of these groups, as shown in Figure 3B, yielded 126.62. However, when CH_3CN was changed to CD_3CN with $CHCl_3$ as the monomer, the intensity of the hydrocarbon groups of PHC in the ^{1}H-NMR spectrum was significantly reduced, as shown in Figure 3C. Thus, CH_3CN played a significant role as a hydrogen atom supplier. With $CDCl_3$ and CD_3CN used, as shown in Figure 3D, the intensity of the "hydrocarbon region" was smaller than that of the ^{1}H-NMR spectrum in Figure 3C. The integration of the hydrocarbon region in Figures 3C and 3D yielded 51.74 and 37.99, respectively.

The participation of CH_3CN was confirmed by deuterium NMR (^{2}H-NMR) (please see Figure S7). When $CDCl_3$ was used instead of $CHCl_3$, a deuterated carbon peak was barely observed in the hydrocarbon region as shown in Figure S7A; however, as shown in Figures S7B and S7C, when CH_3CN was changed to CD_3CN, significant peaks at 2.10 ppm were observed. ^{2}H-NMR generally shows a similar NMR pattern to ^{1}H-NMR, but the signal-to-noise ratio (SNR) of ^{2}H-NMR is much lower compared with that of

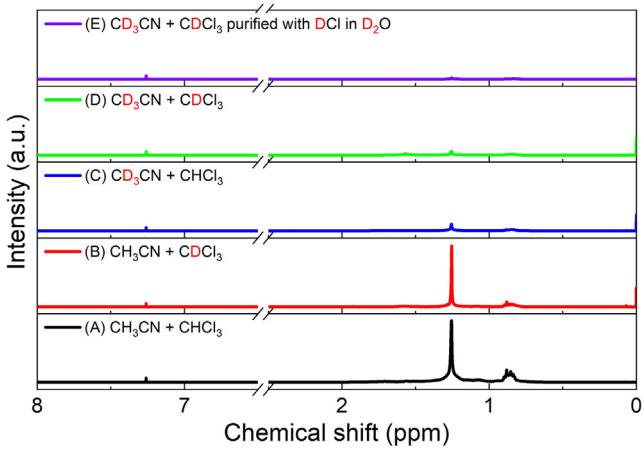

Figure 3. ^{1}H-NMR spectra of PHCs for identification of the termination process

^{1}H-NMR spectra of PHCs synthesized by (A) CH_3CN + $CHCl_3$, (B) CH_3CN + deuterated chloroform ($CDCl_3$), (C) deuterated acetonitrile (CD_3CN) + $CHCl_3$, (D) CD_3CN + $CDCl_3$, and (E) CD_3CN + $CDCl_3$ purified with deuterium chloride (DCl) in deuterium oxide (D_2O).

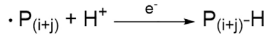

Scheme 5. Termination process of the formed oligomer or polymer by hydrogen atoms

^{1}H-NMR.[53] Therefore, although the deuterated carbon peak did not show peak positions clearly assignable as hydrocarbon (group) peaks, ^{2}H-NMR showed that CH_3CN is the main hydrogen supplier to the PHC product. With $CDCl_3$ and CD_3CN used (Figure 3D), the small value obtained from the integration of the hydrocarbon region indicates that there were other candidates for the hydrogen atom supplier.

In an attempt to determine the effect of HCl(aq), purification was performed using deuterium chloride DCl(aq) in deuterium oxide (D_2O), as shown in Figure 3E. We synthesized PHC using CD_3CN and $CDCl_3$ and purified it using a DCl aqueous solution; the obtained hydrocarbon peak region was much smaller than that obtained using HCl(aq): with the integration of the hydrocarbon region, it is 12.77. This means that HCl(aq), as a hydrogen atom supplier, helped terminate the reaction. The final candidate (that we can think of) is moisture in the air. Figure S8 shows the ^{1}H-NMR spectra for the extracted solutions collected before the start of the reaction (black line), immediately after the electrochemical polymerization (red line), and after exposure to air for 30 min post the reaction (blue line). The CH_3CN peak at 1.94 ppm broadened due to paramagnetic compounds (Knight shift),[54] and there was no change in the peak position despite exposure to air. Based on all of these NMR results, CH_3CN is a main hydrogen atom supplier, except for the hydrogen already present in $CHCl_3$, in the electrochemical polymerization for the synthesis of PHC, and other HCl(aq) also contributes hydrogen atoms in terminating the reaction.

Calculation of carbon participation percentage for $CHCl_3$ and CH_3CN

In addition, carbon participation (as a percentage) could be calculated using the SNR in the quantitative ^{13}C-NMR spectra because carbon has little difference in atomic mass ratio between ^{12}C and ^{13}C, so the reaction rate is not greatly influenced.[55,56] ^{13}C is present at ~1.1 atom % in nature. $^{13}CHCl_3$ was used to synthesize 10 and 99 atom % ^{13}C PHC, and quantitative ^{13}C-NMR analysis was performed under the same NMR conditions, including the same concentration (see Figure S9). The SNR depends on the concentration of the ^{13}C in the PHC samples and the NMR protocols: as noted, the number of scans and external magnetic fields were identical. The SNR values at 1.1, 10, and 99 atom % ^{13}C labeling were 109.14, 984.03, and 9,733.54, respectively, when the SNR was calculated based on the strongest peak at 29.93 ppm. The participation of $CHCl_3$ and CH_3CN for carbon atoms in the PHC was 98.30% and 1.70%, respectively, compared with the 1.1 and 10 atom % ^{13}C PHC samples. Comparing the 1.1 and 99 atom % ^{13}C PHC samples showed that the carbon participation was 98.31% $CHCl_3$ and 1.69% CH_3CN. Thus, approximately 98.3% of the carbon atoms in the products are from $CHCl_3$, and the remainder are from CH_3CN (see Note S1 for additional details). As mentioned above, most of the hydrogen atoms in PHC products came from CH_3CN. The termination scheme is as displayed in Scheme 5.

This explains the termination of electrochemical polymerization by several hydrogen suppliers.

To summarize, as shown in Figure 4, it was found that as the SS316 anode was oxidized, the current increased in the reaction solution. The CH_3CN promoted the termination process of PHC synthesis by deprotonation at the anode. The protons,

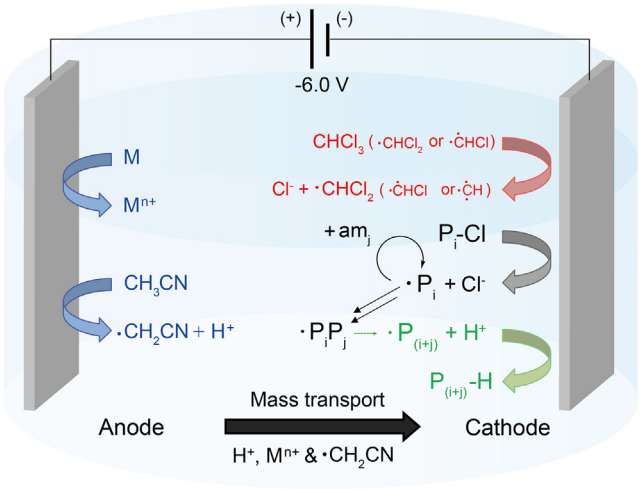

Figure 4. Schematic illustration of the electrochemical polymerization using $CHCl_3$ and CH_3CN with $LiPF_6$

M is a metal compound released from SS316 (M = Fe, Ni, and Mo), and H^+ is a proton. Propagated segments are represented by P. Activated monomers, which have radicals, are represented by am (*i*, *j*, and *n* = integer).

metal ions from the SS316 anode, and dissociated CH_3CN molecules were transported to the cathode by stirring the solution. As the C–Cl bonds of the chlorinated methanes were cleaved on the cathode, the reduction occurred by generating activated monomers; thus, the propagation proceeded by the activated monomers reacting with each other. Finally, the hydrogen atoms contributed by CH_3CN and HCl(aq) helped to terminate the reaction.

In summary, we studied the electrochemical polymerization of chlorinated methanes using isotope-labeled chemicals and electrochemical analysis combined with FT-IR and NMR. CV and NMR analyses showed that the oxidation process involves H atoms coming from CH_3CN and the release of metal ions from the SS316 electrodes at the anode. In addition, the CV curves showed that the C–Cl covalent bonds in the monomers were cleaved during the initiation process at the cathode. We observed that the intensity of the C-H stretch region (peaks for different functional groups C_xH_y) in the FT-IR spectra gradually increased according to the reaction time, and NMR results on timed extractions of the reaction solution agreed with group number ratios from the FT-IR spectra. Our prior studies on the synthesis of PHCs showed that the stoichiometry of PHC from $CHCl_3$ monomer was close to that of CH_2[23]; here, the origin of the hydrogen atoms was identified through ^{1}H-NMR analyses by using CD_3CN, $CDCl_3$, and DCl(aq). CD_3CN yielded a large decrease in the integrated peak area of the hydrocarbon region in the ^{1}H-NMR spectra: CH_3CN is a significant hydrogen atom donor. Additionally, HCl(aq), used for purification after electrochemical synthesis of the PHC, also provides H atoms on the periphery of the PHC, as further assessed by purification by DCl (in D_2O). Therefore, hydrogen atoms came from CH_3CN, $CHCl_3$, and HCl(aq). Most of the carbon in the PHC product came from $CHCl_3$, elucidated from studies of ^{13}C-labeled PHCs. We discovered several aspects of how PHC grows and evolves in this type of electrochemical polymerization using CV, NMR, and FT-IR data together with isotopic labeling of $CHCl_3$ ($CDCl_3$ and $^{13}CHCl_3$) and the acetonitrile solvent. Our approaches should be useful to others who want to understand the time evolution of the growth of polymers by electrochemical polymerization.

EXPERIMENTAL PROCEDURES

Resource availability

Lead contact

Further information and requests for resources should be directed to and will be fulfilled by the lead contact, Rodney S. Ruoff (rsruoff@ibs.re.kr or ruofflab@gmail.com).

Materials availability

All materials generated in this study are available from the lead contact .

Data and code availability

Any requests related to data will be fulfilled by the lead contact upon reasonable request.

Chemicals and characterization

$LiPF_6$ (battery grade, ≥99.99% trace metal basis; Sigma Aldrich) was used as received. CH_2Cl_2 (≥99.5%; Daejung) and CCl_4 (≥99.5%, anhydrous; Sigma-Aldrich) were used as received. $CHCl_3$ (≥99%, containing amylenes as a stabilizer; Sigma-Aldrich) and anhydrous acetonitrile (CH_3CN) (99.8%; Sigma-Aldrich) were purified using a solvent purifier from Vacuum Atmospheres Company before use. $CDCl_3$, acetonitrile-d_3 (CD_3CN), and deuterium chloride (DCl) (35 wt % in D_2O, ≥99 atom % D) were purchased from Sigma-Aldrich. $^{13}CHCl_3$ (99%) was purchased from Cambridge Isotope Laboratories. HCl (37%, Sigma-Aldrich) was used during the purification in the synthesis process. SS sheets (SS316; KwangEun) were washed with acetone, isopropyl alcohol, and deionized (DI) water and dried at 80°C in an air oven for 24 h before use. Silica gel 60 (0.040–0.063 mm; Merck) was used for column chromatography.

CV and CA results were obtained using a Gamry Reference 600+ system. The potential range from 0.00 to −6.00 V (and +6.00 V) was applied to the solution with a 10 mV/s scan rate using an $Ag/AgNO_3$ reference electrode and SS316 working and counter electrodes. ^{1}H-NMR and ^{13}C-NMR spectra were recorded using a Bruker Ascend 400 spectrometer (400 MHz). Chloroform-d ($CDCl_3$) was used as the NMR solvent for ^{1}H- and ^{13}C-NMR experiments. The ^{1}H-NMR spectra were calibrated using a residual non-deuterated solvent shift ($CHCl_3$ = 7.26 ppm), and the ^{13}C-NMR spectra were calibrated using a solvent chemical shift ($CHCl_3$ = 77.16 ppm). FT-IR spectra were obtained using an Agilent 600 series spectrometer in the transmittance mode. XPS was done using a Thermo Scientific ESCALAB 250Xi instrument.

Electrochemical polymerization

All reactions were performed inside an argon-filled glove box. The electrochemical cell was composed of working, counter, and reference electrodes. The area of the cathode and anode is 4 × 4 cm^2, and the thickness of these electrodes is 0.9 mm. The surface-to-volume (S/V) ratio of the electrode is 2.3 mm^{-1}. The distance between the electrodes is 3 cm. The reference electrode was an $Ag/AgNO_3$ non-aqueous reference electrode. Chlorinated monomer solutions (6.2 M) in CH_3CN were prepared in the presence of 23 mmol $LiPF_6$ as the electrolyte. Electrochemical polymerization was conducted at −6.00 V (direct current) for 24 h at room temperature. The insoluble material was removed via vacuum filtration. The residual solvents in the filtered solution were evaporated using a rotary evaporator, and the dried raw product was dissolved in $CHCl_3$ (100 mL). The solution was washed with 3.7% diluted HCl (100 mL × 5 times) using a separation funnel. After drying the

washed solution, the obtained product was purified using silica column chromatography. $CHCl_3$ was used as an eluent.

CV measurement

The potential in the cyclic voltammograms of each chlorinated monomer was swept from 0.00 to −6.00 V, or from 0.00 to 6.00 V, at a scan rate of 10 mV/s at room temperature.

Extraction of solution in the electrochemical reaction and sampling for FT-IR and NMR

Electrochemical reactions were conducted in a glove box. A solution sample (1 mL) was extracted from a point close to the working electrode based on the reaction time. For FT-IR spectroscopy, KBr pellets were prepared in advance and immersed in the extracted solution for 1 min. FT-IR spectra were measured immediately after being pulled out of the glove box. After mixing 0.1 mL extracted solution (0.7 mL with $CDCl_3$ and the NMR solvent [δ = 7.26 ppm]), the impurities were filtered through a syringe filter. The NMR spectra were immediately measured.

SUPPLEMENTAL INFORMATION

Supplemental information can be found online at https://doi.org/10.1016/j.xcrp.2023.101373.

ACKNOWLEDGMENTS

We appreciate insightful questions and comments from the reviewers of the manuscript. The authors appreciate Prof. Jung-Min Kee at UNIST for his remarks about the H/D kinetic isotope effect. This work was supported by the Institute for Basic Science (IBS-R019-D1).

AUTHOR CONTRIBUTIONS

J.H.S., S.H.L., and R.S.R. conceived the study and designed and analyzed the experiments; J.H.S. synthesized and characterized materials; R.R. contributed to analyzing CV results; J.H.S., S.H.L., and R.S.R. primarily wrote the various manuscript versions; and R.R. contributed to writing and reviewing the manuscripts.

DECLARATION OF INTERESTS

The authors declare no competing interests.

Received: January 2, 2023
Revised: February 17, 2023
Accepted: March 17, 2023
Published: April 7, 2023

REFERENCES

1. Yuan, Y., and Lei, A. (2020). Is electrosynthesis always green and advantageous compared to traditional methods? Nat. Commun. *11*, 802–803.

2. Elgrishi, N., Rountree, K.J., McCarthy, B.D., Rountree, E.S., Eisenhart, T.T., and Dempsey, J.L. (2018). A practical beginner's guide to cyclic voltammetry. J. Chem. Educ. *95*, 197–206.

3. Huang, X., Wang, Z., Knibbe, R., Luo, B., Ahad, S.A., Sun, D., and Wang, L. (2019). Cyclic voltammetry in lithium–sulfur batteries—challenges and opportunities. Energy Technol. *7*, ente.201801001.

4. Isse, A.A., Sandonà, G., Durante, C., and Gennaro, A. (2009). Voltammetric investigation of the dissociative electron transfer to polychloromethanes at catalytic and non-catalytic electrodes. Electrochim. Acta *54*, 3235–3243.

5. Durante, C., Isse, A.A., Sandonà, G., and Gennaro, A. (2009). Electrochemical hydrodehalogenation of polychloromethanes at silver and carbon electrodes. Appl. Catal. B Environ. *88*, 479–489.

6. Isse, A.A., Lin, C.Y., Coote, M.L., and Gennaro, A. (2011). Estimation of standard reduction potentials of halogen atoms and alkyl halides. J. Phys. Chem. B *115*, 678–684.

7. Labaye, D.-E., Jérôme, C., Geskin, V.M., Louette, P., Lazzaroni, R., Martinot, L., and Jérôme, R. (2002). Full electrochemical synthesis of conducting polymer films chemically grafted

to conducting surfaces. Langmuir *18*, 5222–5230.

8. Little, R.D., and Moeller, K.D. (2018). Introduction: electrochemistry: Technology, synthesis, energy, and materials. Chem. Rev. *118*, 4483–4484.

9. Martínez-Huitle, C.A., and Ferro, S. (2006). Electrochemical oxidation of organic pollutants for the wastewater treatment: direct and indirect processes. Chem. Soc. Rev. *35*, 1324–1340.

10. Sandford, C., Edwards, M.A., Klunder, K.J., Hickey, D.P., Li, M., Barman, K., Sigman, M.S., White, H.S., and Minteer, S.D. (2019). A synthetic chemist's guide to electroanalytical tools for studying reaction mechanisms. Chem. Sci. *10*, 6404–6422.

11. Stephen, H.R., Schotten, C., Nicholls, T.P., Woodward, M., Bourne, R.A., Kapur, N., and Willans, C.E. (2020). Development, A versatile electrochemical batch reactor for synthetic organic and inorganic transformations and analytical electrochemistry. Org. Process Res. Dev. *24*, 1084–1089.

12. Minteer, S.D., and Baran, P. (2020). Electrifying synthesis: recent advances in the methods, materials, and techniques for organic electrosynthesis. Acc. Chem. Res. *53*, 545–546.

13. Schäfer, H.J. (2011). Contributions of organic electrosynthesis to green chemistry. Compt. Rendus Chem. *14* (7-8), 745–765.

14. Simionescu, C., Cianga, I., Ivanoiu, M., Duca, A., Cocarla, I., and Grigoras, M. (1999). Synthesis and electrochemical polymerization of some monomers with Schiff base or vinylene structures and thiophene moieties. Eur. Polym. J. *35*, 587–599.

15. Bhadani, S.N., Ansari, Q., and Gupta, S.K.S. (1992). Electrochemical polymerization of acrylonitrile with quaternary salts. J. Appl. Polym. Sci. *44*, 121–126.

16. Maiti, S., Das, D., and Sen, K. (2012). Electrochemical polymerization of pyrrole: key process control parameters. J. Electrochem. Soc. *159*, E154–E158.

17. Sari, B., Talu, M., and Yildirim, F. (2002). Electrochemical polymerization of aniline at low supporting-electrolyte concentrations and characterization of obtained films. Russ. J. Electrochem. *38*, 707–713.

18. Endo, K., and Bu, H.-B. (2001). Synthesis of disulfide polymer by electrochemical polymerization of α, ω-alkanedithiols. Polymer *42*, 3915–3918.

19. Nur, Y., Pitcher, M.W., Seyyidoğlu, S., and Toppare, L. (2008). Facile synthesis of poly (hydridocarbyne): a precursor to diamond and diamond-like ceramics. J. Macromol. Sci., Part A *45* (5), 358–363.

20. Xu, L., Yao, X., Khan, A., and Mavrikakis, M. (2016). Chloroform hydrodechlorination over palladium–gold catalysts: a first-principles DFT study. ChemCatChem *8*, 1739–1746.

21. Sonoyama, N., Hara, K., and Sakata, T. (1997). Reductive electrochemical decomposition of chloroform on metal electrodes. Chem. Lett. *26*, 131–132.

22. Lei, C., Liang, F., Li, J., Chen, W., and Huang, B. (2019). Electrochemical reductive dechlorination of chlorinated volatile organic compounds (Cl-VOCs): effects of molecular structure on the dehalogenation reactivity and mechanisms. Chem. Eng. J. *358*, 1054–1064.

23. Seo, J.H., Nam, H.J., Buyukcakir, O., Rajendiran, R., Seong, W.K., Jiang, Y., Kim, M.H., Lee, S.H., and Ruoff, R.S. (2022). Continuous production of hyperbranched polyhydrocarbons by electrochemical polymerization of chlorinated methanes. Polym. Chem. *13*, 5781–5788.

24. Lee, S.H., Seo, J.H., Shin, E., Joo, S.H., Buyukcakir, O., Jiang, Y., Kim, M., Nam, H., Kwak, S.K., and Ruoff, R.S. (2022). Structural analysis of hyperbranched polyhydrocarbon synthesized by electrochemical polymerization. Polym. Chem. *13*, 5309–5315.

25. Plekhanov, V.P., Tsyganok, A.I., and Kulikov, S.M. (1995). Electrochemical reductive dehalogenation of chlorobenzenes. Russ. Chem. Bull. *44*, 1091–1095.

26. Jalil, A.A., Triwahyono, S., Razali, N.A.M., Hairom, N.H.H., Idris, A., Muhid, M.N.M., Ismail, A., Yahaya, N.A.M., Ahmad, N.A.L., and Dzinun, H. (2010). Complete electrochemical dechlorination of chlorobenzenes in the presence of various arene mediators. J. Hazard Mater. *174*, 581–585.

27. Rodrigues, R., Betelu, S., Colombano, S., Tzedakis, T., Masselot, G., and Ignatiadis, I. (2020). In situ chemical reduction of chlorinated organic compounds. In Environmental Soil Remediation and Rehabilitation (Springer), pp. 283–398.

28. Isse, A.A., Huang, B., Durante, C., and Gennaro, A. (2012). Electrocatalytic dechlorination of volatile organic compounds at a copper cathode. Part I: polychloromethanes. Appl. Catal. B Environ. *126*, 347–354.

29. Durante, C., Huang, B., Isse, A.A., and Gennaro, A. (2012). Electrocatalytic dechlorination of volatile organic compounds at copper cathode. Part II: polychloroethanes. Appl. Catal. B Environ. *126*, 355–362.

30. Isse, A.A., Gottardello, S., Durante, C., and Gennaro, A. (2008). Dissociative electron transfer to organic chlorides: electrocatalysis at metal cathodes. Phys. Chem. Chem. Phys. *10*, 2409–2416.

31. Nur, Y., Cengiz, H.M., Pitcher, M.W., and Toppare, L.K. (2009). Electrochemical polymerization of hexachloroethane to form poly (hydridocarbyne): a pre-ceramic polymer for diamond production. J. Mater. Sci. *44*, 2774–2779.

32. Nur, Y., Duygulu, Ş., Pitcher, M.W., and Toppare, L. (2012). The electrochemical synthesis of poly (methylcarbyne) for diamond film coatings. J. Appl. Polym. Sci. *124*, 3626–3632.

33. Blanc, F., Leskes, M., and Grey, C.P. (2013). In situ solid-state NMR spectroscopy of electrochemical cells: batteries, supercapacitors, and fuel cells. Acc. Chem. Res. *46*, 1952–1963.

34. Pecher, O., Bayley, P.M., Liu, H., Liu, Z., Trease, N.M., and Grey, C.P. (2016). Automatic Tuning Matching Cycler (ATMC) in situ NMR spectroscopy as a novel approach for real-time investigations of Li-and Na-ion batteries. J. Magn. Reson. *265*, 200–209.

35. Pecher, O., Vyalikh, A., and Grey, C.P. (2016). In Challenges and new opportunities of in situ NMR characterization of electrochemical processes, AIP Conference Proceedings (AIP Publishing LLC), 020011.

36. Kato, Y., and Noguchi, T. (2016). Imaging, FTIR spectroelectrochemistry combined with a light-induced difference technique: application to the iron-quinone electron acceptor in photosystem II. Biomed. Spectrosc. Imag. *5*, 269–282.

37. Huang, L., Sun, J.-Y., Cao, S.-H., Zhan, M., Ni, Z.-R., Sun, H.-J., Chen, Z., Zhou, Z.-Y., Sorte, E.G., Tong, Y.J., and Sun, S.G. (2016). Combined EC-NMR and in situ FTIR spectroscopic studies of glycerol electrooxidation on Pt/C, PtRu/C, and PtRh/C. ACS Catal. *6*, 7686–7695.

38. Krtil, P., Kavan, L., and Novák, P. (1993). Oxidation of acetonitrile-based electrolyte solutions at high potentials: an in situ fourier transform infrared spectroscopy study. J. Electrochem. Soc. *140*, 3390–3395.

39. Zheng, H., Li, K., Cody, G.D., Tulk, C.A., Dong, X., Gao, G., Molaison, J.J., Liu, Z., Feygenson, M., Yang, W., et al. (2016). Polymerization of acetonitrile via a hydrogen transfer reaction from CH3 to CN under extreme conditions. Angew. Chem. Int. Ed. Engl. *55*, 12040–12044.

40. Becker, J.Y., and Koch, T.A. (1994). Electrochemical reduction of unsaturated nitriles in acetonitrile and nitromethane. Electrochim. Acta *39*, 2067–2071.

41. He, T.-J., Ye, Z., Ke, Z., and Huang, J.-M. (2019). Stereoselective synthesis of sulfur-containing β-enaminonitrile derivatives through electrochemical Csp3–H bond oxidative functionalization of acetonitrile. Nat. Commun. *10*, 833–839.

42. Ward Jones, S.E., Chevallier, F.G., Paddon, C.A., and Compton, R.G. (2007). General theory of cathodic and anodic stripping voltammetry at solid electrodes: mathematical modeling and numerical simulations. Anal. Chem. *79*, 4110–4119.

43. Achterberg, E.P., Gledhill, M., and Zhu, K. (2018). Voltammetry—Cathodic Stripping. Reference Module in Chemistry, Molecular Sciences and Chemical Engineering (Elsevier).

44. Jiang, F., Yang, S., Liu, H., Cheng, X., Liu, L., Xiang, R., Zhang, Q., Kaskel, S., and Huang, J. (2021). Mechanism understanding for stripping electrochemistry of Li metal anode. SusMat *1*, 506–536.

45. Lohrberg, O., Maletti, S., Heubner, C., Schneider, M., and Michaelis, A. (2022). Understanding Li plating and stripping behavior in zero-excess Li metal batteries using operando dilatometry. J. Electrochem. Soc. *169*, 030543.

46. Shiga, T., Masuoka, Y., and Nozaki, H. (2021). Observation of lithium stripping in super-concentrated electrolyte at potentials lower than regular Li stripping. RSC Adv. *11*, 13359–13365.

47. Yoon, G., Moon, S., Ceder, G., and Kang, K. (2018). Deposition and stripping behavior of lithium metal in electrochemical system: continuum mechanics study. Chem. Mater. *30*, 6769–6776.

48. Kock, L.D., Lekgoathi, M.D.S., Crouse, P.L., and Vilakazi, B.M. (2012). Solid state vibrational spectroscopy of anhydrous lithium hexafluorophosphate ($LiPF_6$). J. Mol. Struct. *1026*, 145–149.

49. Bertini, I., Luchinat, C., and Parigi, G. (2002). Magnetic susceptibility in paramagnetic NMR. Prog. Nucl. Magn. Reson. Spectrosc. *40*, 249–273.

50. Febrian, R., Roddy, J.P., Chang, C.H., Devall, C.T., and Bracher, P.J. (2021). Removal of paramagnetic ions prior to analysis of organic reactions in aqueous solutions by NMR spectroscopy. ACS Omega *6*, 14727–14733.

51. Atkins, P., and Julio, D.P. (2006). Atkins' Physical Chemistry (Oxford University Press), pp. 286–288.

52. Laidler, K.J. (1987). Chemical Kinetics (Harper & Row).

53. Mantsch, H.H., Saitô, H., and Smith, I.C. (1977). Deuterium magnetic resonance, applications in chemistry, physics and biology. Prog. Nucl. Magn. Reson. Spectrosc. *11*, 211–272.

54. Grey, C.P., and Dupré, N. (2004). NMR studies of cathode materials for lithium-ion rechargeable batteries. Chem. Rev. *104*, 4493–4512.

55. Westaway, K.C. (2006). Using kinetic isotope effects to determine the structure of the transition states of S_N2 reactions. Adv. Phys. Org. Chem. *41*, 217–273.

56. Lynn, K.R., and Yankwich, P.E. (1961). Isotope fractionation at the methyl carbon in the reactions of cyanide ion with methyl chloride and methyl bromide. J. Am. Chem. Soc. *83*, 3220–3223.